TAILORED EXPERIMENTS FOR VALIDATION OF CFD WITH FSI FOR NUCLEAR APPLICATIONS

Eric Lillberg, Kristian Angele, Gustav Lundqvist
Department of Fluid Mechanics
Vattenfall AB
eric.lillberg@vattenfall.com; kristian.angele@vattenfall.com; gustav.lundqvist@vattenfall.com

Nicolas Edh
Department of Fluid Mechanics and Mechanical Integrity
Forsmarks Kraftgrupp AB
nsf@forsmark.vattenfall.com

ABSTRACT

The motivation for the following work is related to the numerous problems with Flow Induced Vibrations (FIV) due to Fluid Structure Interaction (FSI) at nuclear power plants [1].Such vibration problems are very important since they are related to the safety and the availability of the plants. To predict and avoid potential problems in the future it is required to have advanced tools, i.e. Computational Fluid dynamics (CFD) simulations with FSI.

For this purpose two experiments have been designed to provide relevant data for validation of CFD with FSI. These simplified test cases have been designed specifically for the purpose of CFD validation in such that the geometry is simple (facilitates meshing), the boundary conditions are well known and the vibration mechanisms covers both free vibration and fluid elastic response. The direct practical relevance of these two cases are in-core monitoring system and fuel rod vibrations due to external loads, e.g. earth quake and LOCA, but the investigated mechanisms can be extended to many types of FIV situations including leakage flow vibrations and buffeting.

The first experiment considers the free vibration of a slender prismatic beam with rectangular cross section in axial flow. The vibration and the damping from the fluid is investigated using laser distance meters at different flow velocities. The second experiment consists of a cross shaped narrow flow path with a centered cylindrical thin-walled rod subjected to axial flow. The resulting fluid elastic response of the rod is investigated and the modes of vibration, amplitude and damping is measured using simultaneous particle tracking velocimetry (PTV) and pressure measurements.

KEYWORDS
CFD, FSI, Validation, Nuclear, Experiments

1. INTRODUCTION

The motivation for the following work is related to the numerous problems with Flow Induced Vibrations (FIV) in nuclear power plants (NPPs) [1]. Such vibration problems are very important since they are related to the safety and the availability of the plants. To predict and avoid potential problems in the future advanced tools like computational fluid dynamics (CFD) with fluid structure interaction (FSI)

could be used. For this purpose experimental validation of CFD with FSI is necessary and two simple and idealized test cases have been designed for this purpose.

Flow induced vibrations is an important phenomenon in the design of fluid conveying systems and components subjected to external or internal flow. As the structure response to the fluid forcing grows in amplitude the motion of the structure itself changes the flow pattern and the resulting loading significantly and a fluid structure interaction is created. In order to asses FSI phenomena computational fluid mechanics is an important tool. Due to the strong coupling the simultaneous calculation of both the transient fluid load and the structural response is necessary. Recent development of computational software for coupled fluid/structure analyses has made it possible to address transient flows and complex geometry for industrial applications.

However, the lack of experimental data for benchmarking of available computational tools makes coupled calculations an option that is most often not considered for industrial applications. The current experiments proposed in this report are designed to create well-defined data for relevant industrial applications.

Examples of the practical relevance of the presented experiments are structural integrity of RPV internals e.g. fuel rods, guide tubes and small bore piping due to external loads, e.g. fluid transients, earth quake and LOCA. The flow induced vibration and fluid damping of the structures by the surrounding water is highly relevant as it will strongly affect the resulting stresses in the component.

2. EXPERIMENTAL SETUPS

In the first experimental setup the damping of free rod vibrations by water flow is studied. The experimental setup consists of a square Plexiglas test-section (for visual access) with the inner dimensions 80 mm x 80 mm, see Figure 1. A slender, rectangular stainless steel rod (cross section dimensions: 20 mm x 8 mm, ±0.1 mm, and length L=1500 mm) is placed in the center of the test section, with a fixed bottom-end and pinned top-end. A flow straightener and perforated plates assures a homogenous flow profile at the inlet of the test section.

Upstream the test section is connected to a pump and flow meters and downstream to a reservoir with constant water level, c.f. Figure 1. A mechanism for pulling the rod in its weak direction by a thread at the middle position of the rod was used as seen in the right hand picture of Figure 1. The string is tensioned using a micrometer screw and the displacement of the rod is checked before the string is cut by using a razor blade, which allows for a well-defined release of the rod.

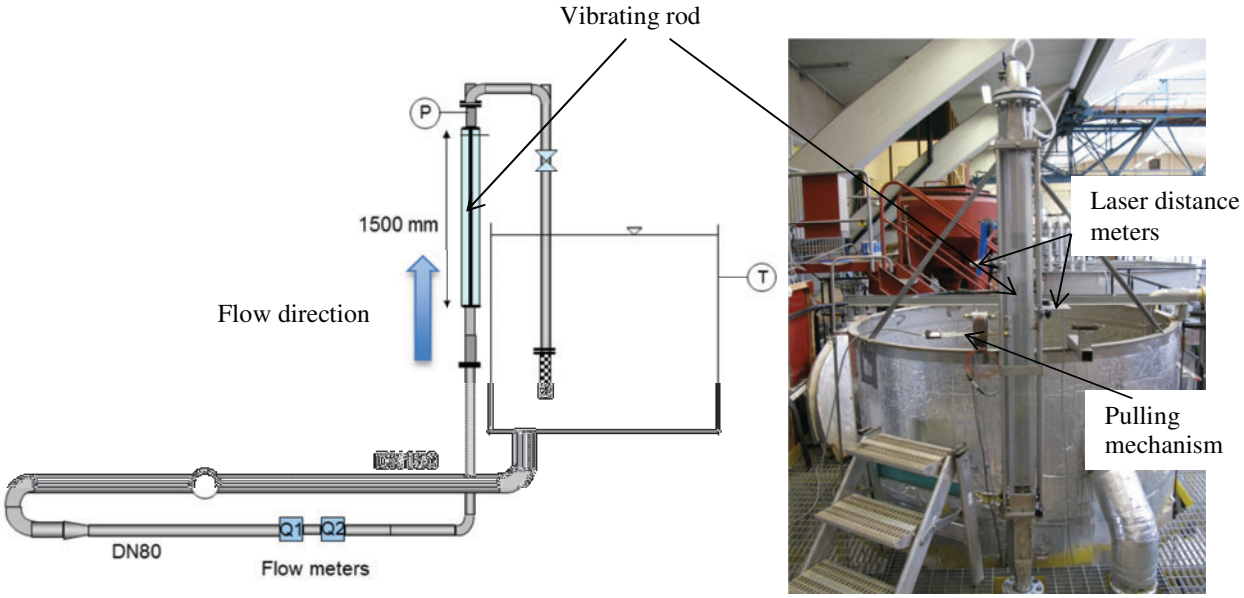

Figure 1: Experimental setup for study of damping of free rod vibrations

In the second experimental setup an important part of a nuclear in-core neutron flux monitoring system is considered. The Average Power Range Monitor (APRM) system consists of a number of in-core neutron flux detectors that are positioned axially inside guide tubes located in-between the fuel bundles, see Figure 2.

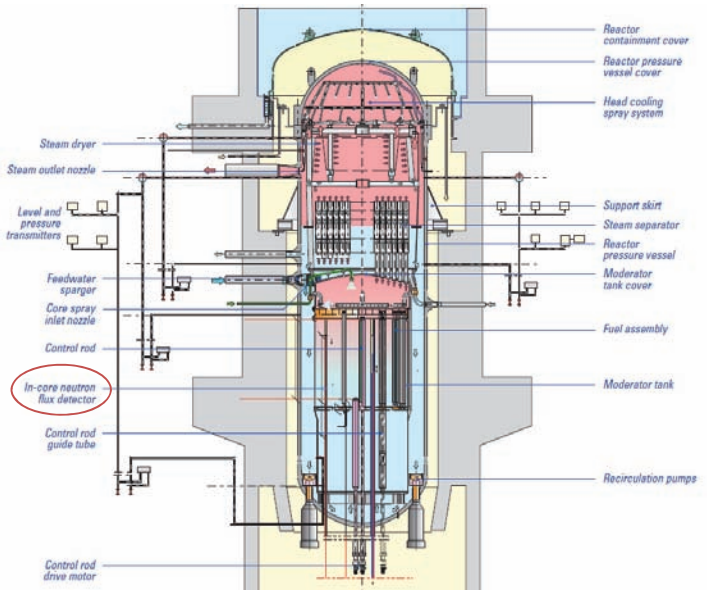

Figure 2: Section of a BWR showing the location of the in-core neutron flux detector system

In this section in-between the fuel boxes the bypass water, approximately 13-15% of the total flow in the main recirculation loop, flows axially upwards along the guide tube outer surface in the channel formed between four fuel boxes. The guide tube is only 19 mm in diameter and 4040 mm tall which makes it weak and susceptible to fluid forces. The flow path between the corner of the fuel boxes and the guide tube is only 6 mm wide so even small deflections of the guide tube from its cantered position will significantly alter the shape of the flow path and the resulting forcing on the guide tube, see Figure 3.

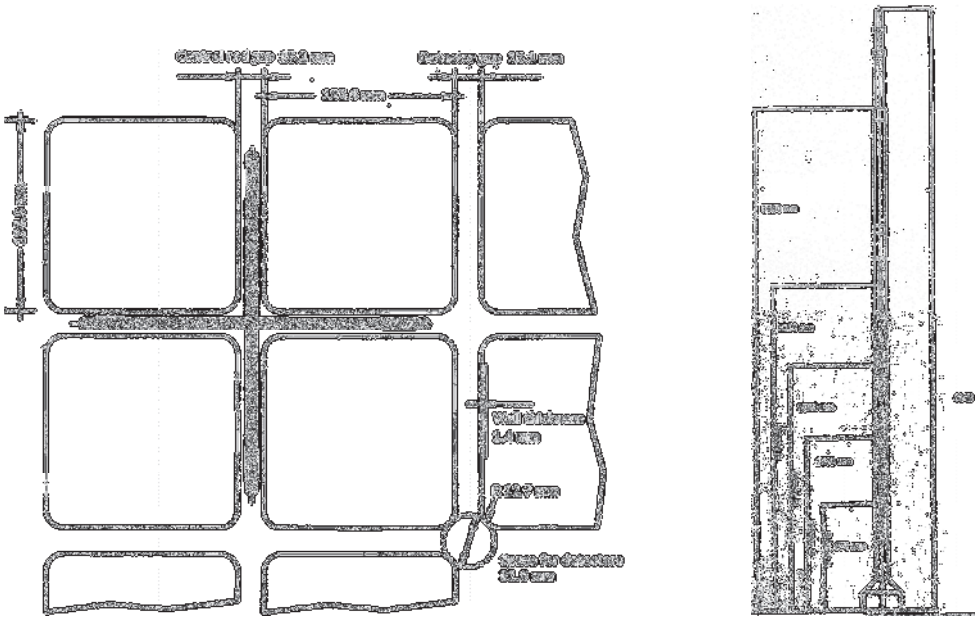

Figure 3: Schematic of the fuel boxes and guide tube position (left) and dimensions (right)

The lower end of the guide tube is fixed in the core support plate while the upper end is fastened in the core grid with a spring. The resulting mechanical system typically has a fundamental frequency in the range of 2-3 Hz.

For a large boiling water reactor (BWR) the bypass flow is as large as 1000-1800 kg/s divided into 125-169 channels, one for each super cell (four fuel bundles) in the core. With an average density ρ = 762 kg/m^3 at a temperature of T = 286 ºC the resulting average flow velocity is in the range of 2 m/s.

Scaling of the experimental setup is necessary due to the limited length of the available test section. The length of the in-core neutron flux detector tube is 4040 mm and the test section is 1500 mm long which gives a length ratio of 0.37. In order to get a good frequency resolution for the vibration measurements the natural frequency of the test tube should be as low as possible and therefore the diameter and wall thickness of the test tube is decreased compared to the real housing tube. The fundamental frequency, f_{s0} for a beam with uniformly distribute mass is given by equation (1)[3]

$$f_{s0} = \frac{1}{2\pi}\frac{C}{L^2}\sqrt{\frac{EI}{\rho_s}} \tag{1}$$

Where E is the Young's modulus, L is the tube length, I is the area moment of inertia and ρ_s is the mass density (mass/length). For "fixed-pinned" and "fixed-free" boundary conditions the constant is C=15.418 and C=3.5156 respectively. The area moment of inertia for a thin wall tube is $I = \pi/4(r_{outer}^4 - r_{inner}^4)$ where $r_{outer/inner}$ is the outer and inner radius respectively.

The real life detector housing tube is 19 mm in diameter, the channel width is 15.1 mm and the fuel bundle corner radius is 12.7 mm. Scaling with the 8 mm diameter test tube the fuel bundle corner radius is 5.4 mm and channel width 6.4 mm leaving a total space for the test tube equal to the area of a 13.4 mm diameter circle. The resulting geometry in the 80x80 mm test section is shown in Figure 4.

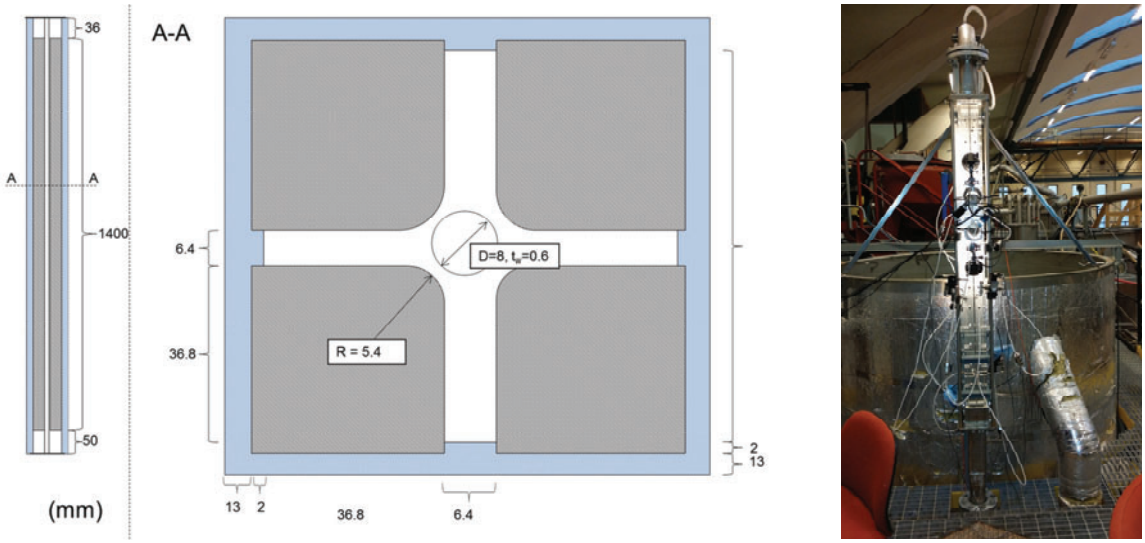

Figure 4: Left: Dimensions of the scaled test section using 8 mm diameter tube.

Using a stainless steel tube with 8 mm diameter and 0.6 mm wall thickness, E=196 GPa, ρ=7863 kg/m^3, ρ_s=0.11 kg/m and L=1.486 m the "fixed-pinned" fundamental frequencies are then 14.6 Hz.

With smaller tube diameter the channel width need also to be reduced since the tube diameter to channel width ratio together with the flow velocity governs the amplitude and frequency content of the pressure oscillations which should remain similar to the real application. The corner radius of the fuel bundles will also be changed in order to create flow structures similar to the real life application. Also, the narrow channel defines the flow path as the tube moves which affects the boundary layer displacement thickness and the added mass.

The inflow region is defined by the corners of the fuel bundles. The narrow channel between the bundles will act as a contraction reducing any swirl or large scale turbulence in the flow through vortex stretching. A vena-contracta and consequently a small recirculation zone forms at the entrance due to the sharp corners. This can be reproduced with good accuracy by most CFD methods why this situation is preferred. Due to the narrow channels re-laminarisation of the boundary layer might occur at lower flow velocities.

3. MATERIAL PROPERTIES AND BOUNDARY CONDITIONS

The test rod and tube are fixed at its lower end and pinned at the top. The fluid and material properties are given in Table 1.

Table 1: Structure and fluid properties and boundary conditions summary

Property	Value
Rod length (between BCs)	1.486 m
Rod diameter	0.008 m
Rod wall thickness	0.0006 m
Rod density	7863 kg/m^3
Young's modulus	196 GPa
Water density	998 kg/m^3
Temperature	20 ºC

Rod upstream support	Fixed
Rod downstream support	Pinned (Hinged)
Boundary layer	Not tripped
Inflow boundary	Flowrate 0-15 l/s
Outflow boundary	Fixed pressure

The inflow is defined by the flowrate ranging from 0-15 l/s. The outflow boundary and piping is connected to a reservoir at constant pressure.

4. INSTRUMENTATION

4.1. Free rod vibration experiment case

Two laser distance meters one on each side of the rod, c.f. Figure 1, are placed at different vertical positions in order to verify the fundamental vibration mode. The laser distance meters are measuring the position of the rod as a function of time with a temporal resolution of the order of milliseconds and a spatial resolution of the order of 25 µm. The linearity of the calibration confirms the uncertainty, see Figure 5 (left), however the test results indicates that noise becomes similar to the signal at about 70 µm. The sampling frequency used was 1 kHz.

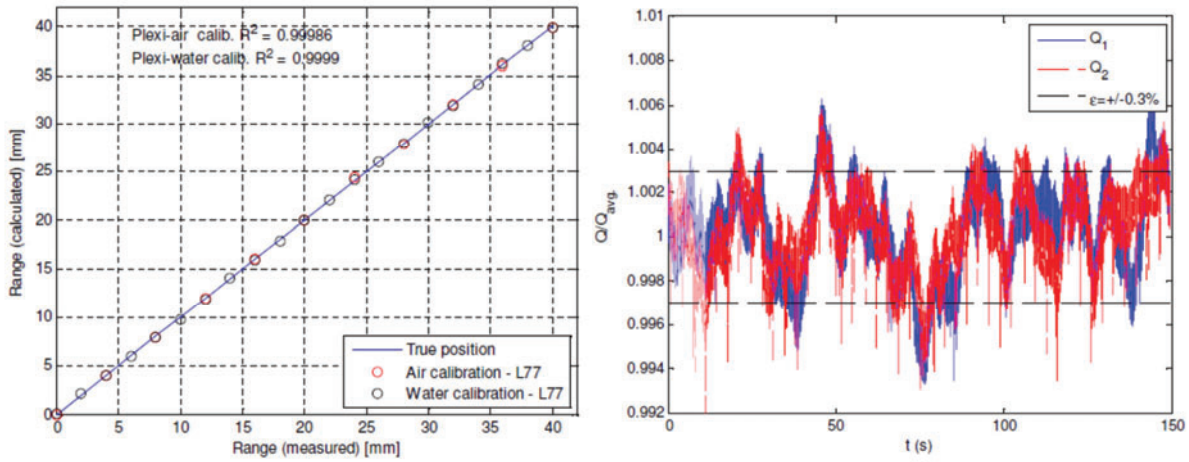

Figure 5: Calibration of the laser distance meters and flow rate accuracy

The flow is provided from the 6 m^3 tank with a free surface in a closed loop using the pump. The pump was regulated by the two electromagnetic flow meters and kept constant throughout a test within an accuracy of 0.3 %, c.f. Figure 5 (right).

The temperature is measured by a Pt-100 sensor with an accuracy of about 0.1-0.2°C and is constant throughout a test. Also the pressure is monitored in the test section with a transducer with an uncertainty of the order of 0.1 %.

4.2. Fluid elastic experimental case

In order to estimate the loading on the tube in the central channel of the experimental setup pressure transducers are placed in the narrow flow path between the tube and the plates forming the corners of the

fuel bundles. Pressure measurements are made at the level of the vibration measurements along the channel. Pressure measurements are made at the locations defined in figure 6.

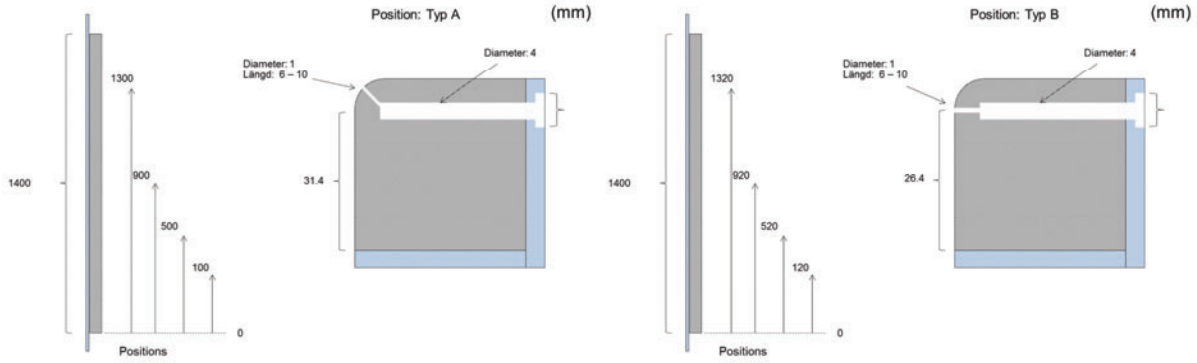

Figure 6: Positions of pressure measurements

The differential pressure transducers used, BD Sensors DMD331, have a range of 100 mbar, an uncertainty ≤ ± 0.5% of Full Scale Output (FSO) (corresponding to 0.5 mbar) and a response time < 5 ms. The positive side of the pressure transducers are connected to the test section with short tubes, < 10 cm, to get a good frequency response and the negative side are collected to a common tube, with a valve, at the same level as the transient pressure measurements. The valve is kept open until the flow rate and static pressure is stabilized and then closed while the transient measurements are made. In this way it was possible to use sensitive differential pressure transducers although the background pressure at some measurement points was as high as 3 bars for the highest flow rates due to the high pressure drop over the test section. The sampling rate of the pressure transducers was set to 1 kHz.

Velocity is measured using electromagnetic flow meters, Krohne Optiflux 4000. The water flow rate is between 0-15 l/s which corresponds to a bulk velocity of approximately 0-15 m/s in the test section. The time variation of the flow is low compared to the frequency of the rod motion and pressure fluctuations. The accuracy of the flow measurements is ≤ ± 0.3 % FSO.

Two high speed cameras, located at 90 degree angle at two different locations along the tube axis, captures the in plane motion in two directions simultaneously. The cameras are synchronized in time using a common trigger. The steel tube is painted black at the measurement locations and white dots are sprayed onto the black surface. The cameras use a 2/3" 2080x1044 pixels CCDs which gives a pixel resolution of 5 µm. As the tube moves the dots are tracked using a Particle Tracking Velocimetry (PTV) algorithm [2]. The favorable dot size for the algorithm is 3-50 pixels. The cameras use tele-centric lenses with 1X magnification, a fixed working distance of 65 mm and the region of interest (ROI) covers 288x100 pixels of the total CCD area. This allows for a frame rate of 750 fps. To establish a relation between the real world coordinates and the measured coordinates of the camera pixels a reference frame was chosen for each camera setup where a predefined distance was correlated to the image of the measurement. This is a source of error in the position measurement which is constant for each camera position and is of the same magnitude as the pixel size ~5 µm.

The accuracy of the PTV algorithm was verified using a "manufactured solution" procedure where computer generated images with particles of different sizes move along prescribed trajectories. By this procedure the accuracy of the algorithm could be established with good precision to within 5 µm or 0.5% of the measurement range. The synchronization signal of the cameras is sampled together with the pressure measurements to create a fully time synchronized coupled data set with pressure loads and the resulting motion. An example of the time synchronized data with in-plane position and pressure is seen in figure 7.

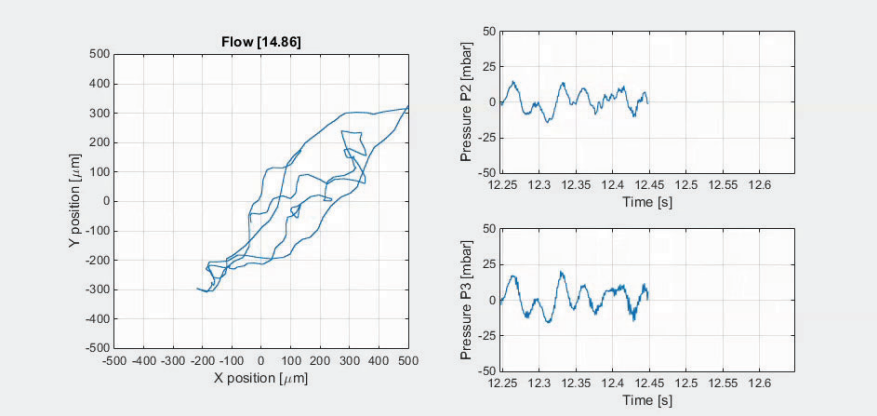

Figure 7: Snapshot of the fully time synchronized data with pressure and in-plane position.

5. RESULTS

Measurements in air and water with no flow rate were performed initially and subsequently tests in water with 1.0 m/s and 3.0 m/s bulk velocity was performed. All measurements were repeated three times to check for repeatability of the results. The effect of the fluid and the flow rate on the frequency and the damping of the rod vibrations were investigated. The initial amplitude of the rod at the position of its maximum was always 10 mm from its original position of equilibrium.
The results below are first displayed as the amplitude as a function of time for all test cases, from the release of the rod at its initial 10 mm position until the rod is at rest, e.g. see Figure 8 for the air test case and for water case with 0, 1 and 3 m/s.

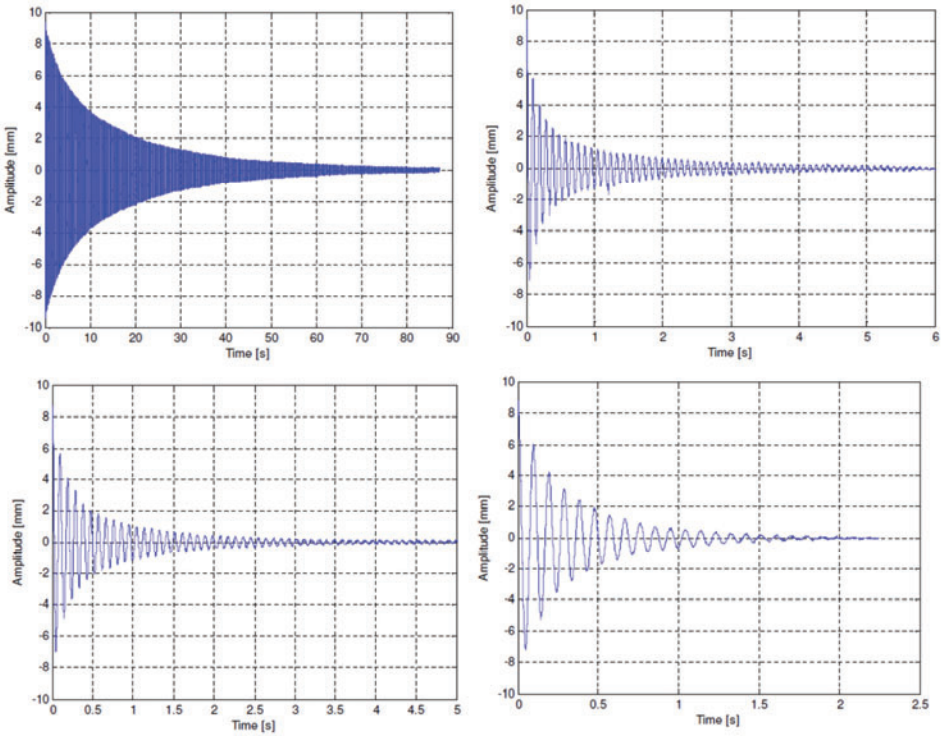

Figure 8: Harmonic oscillation in air (top left), water (top right),
water 1m/s (bottom left) and water 3m/s (bottom right)

In the figure below the absolute values of the rod amplitude are displayed in a logarithmic plot. When displayed in this way one can see that the vibrations of the rod to a large extent constitute a harmonic, periodic oscillation as described by equation (2) below, with a unique damping factor γ, indicated by the full blue line in Figure 9 and a well-defined angular frequency ω. The natural frequency in air is 12.3 Hz while the same frequency in water reduces to 10.7 Hz due to added mass.

$$x = Ae^{-\gamma t}\cos(\omega \cdot t) \tag{2}$$

The resulting damping as a function of flow rate is shown in the bottom right picture of Figure 9.

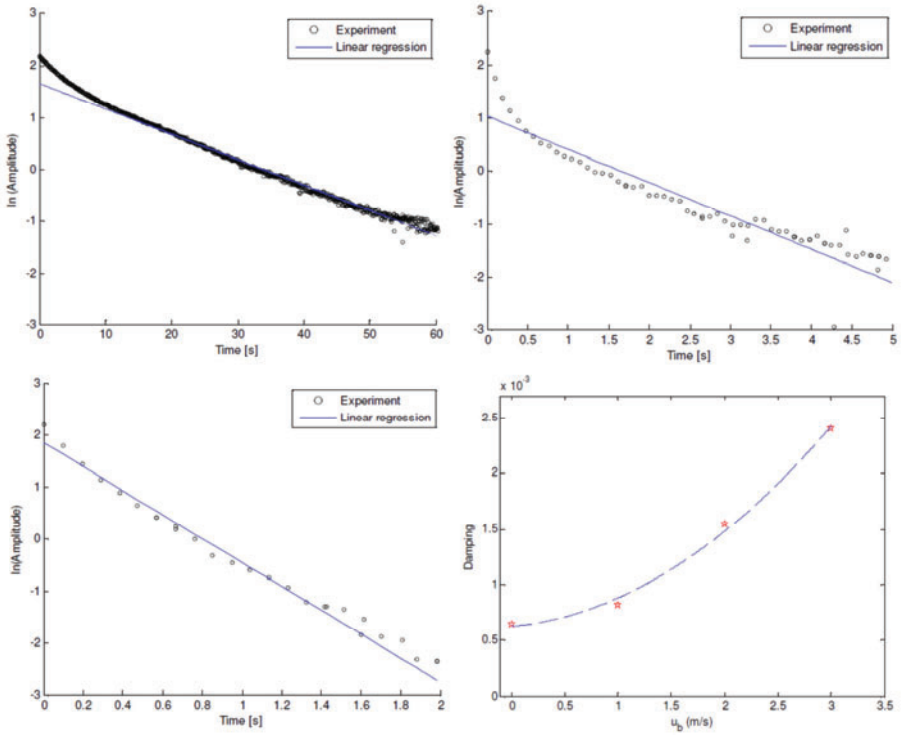

Figure 9: Damping of the harmonic oscillations at air 0 m/s (top left), water 0 m/s (top right), water 3 m/s (bottom left), resulting damping a.f.o. velocity (bottom right)

The structural response in the second experiment is shown in the frequency response at different water flow rates. The response spectra for the tube in air and water with axial flow rates of 0, 5 and 15 l/s are shown in Figure 10.

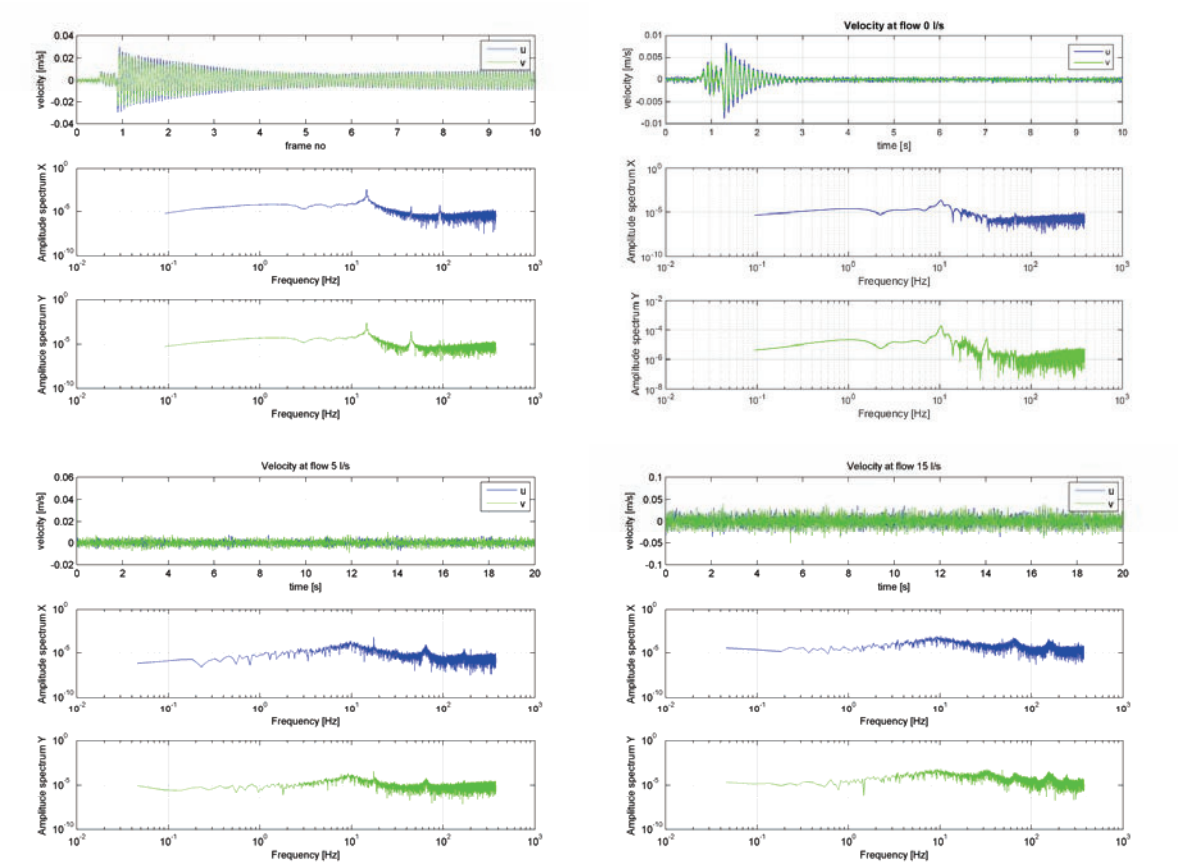

Figure 10: Frequency response of the tube at air 0 l/s (top left), water 0 l/s (top right), water 5 l/s (bottom left), water 15 l/s (bottom right)

As seen in Figure 10 the added mass effect is seen for the 0 m/s runs where water yields a natural frequency of the first bending mode of 10.2 Hz and in air 14.6 Hz. The measurement in air agrees well with the analytic value of 14.6 Hz from equation (1). The measurements for higher water flow rates shows a broad peak at the fundamental frequency but also the higher modes of vibration at different amplitudes depending on flow rate.

6. CONCLUSIONS

The two experimental test cases provides easy yet valuable data for the verification and validation of CFD with FSI. The geometrical configurations are simple and facilitates meshing but still provides a range of physical details that can be investigated by simulations. Boundary conditions are also well defined and accurate which is cardinal for validation of CFD.

The accuracy of the measurements is high and the geometry itself might be the largest source of error in the setups. The fluid elastic case is run in a symmetric configuration which is not optimal from a CFD point of view since the experiments are never as symmetric as a CFD model. Further investigations will include non-symmetric flow configurations.

In this first summary this experimental data is not yet fully analyzed and further insight into the flows and mechanical response will be provided as both CFD/FSI analysis are performed and further experiments are made. No “on-set” was seen in any of the experiments which of course would be an interesting

phenomenon. But nevertheless the data is more similar to the everyday situation of the nuclear engineer working on structural verification of components where the question is not if an “on-set” occurs, since that is unacceptable, but rather what is the maximum amplitude of vibration at the foreseen flow velocities.

ACKNOWLEDGMENTS

The authors wish to acknowledge the energy research corporation Energiforsk AB for funding parts of the experiments.

REFERENCES

1. P. Nilsson, E. Lillberg “Flow Induced Vibrations (FIV) in Swedish NPPs”, **Swedish Radiation safety authority Report**, PENSKI-071025-02 (2002).
2. J. Kristian Sveen: "An introduction to MatPIV v. 1.6.1", **eprint series, Dept. of Math. University of Oslo, "Mechanics and Applied Mathematics"**, NO. 2 ISSN 0809-4403, August 2004
3. Warren C. Young, Richard G. Budynas, “Roark’s Formulas for Stress and Strain”, 7th Edition